

Aristotle University of Thessaloniki  
Faculty of Science  
Department of Physics  
Section of Astrophysics, Astronomy and Mechanics  
Laboratory of Astronomy



Diploma Thesis:

# Discovery probability of transiting extragalactic planets and habitable exoplanet statistics in the Milky Way



Theodoros Anagnos

Supervisor:

Professor John H. Seiradakis

Co-supervisor:

Dr. Dimitris Mislis

Examining Committee:

Professor Manolis Pleionis  
Professor Kleomenis Tsiganis



With data from  
*Isaac Newton Group of Telescopes*

Thessaloniki, September 2014



# Acknowledgements

There are several people without whom you would not be reading this Thesis. Of course I own a lot to my Supervisor Professor John H. Seiradakis (Aristotle University of Thessaloniki-AUTH) for his guidance, his vital ideas on this project and for giving the chance to an undergraduate student to work with professional equipment on real research projects. Most of all I would like to thank him for his kindness and his tolerance on my mistakes and for always being there when he was needed. A simple acknowledgment is not enough for my friend Dimitris Mislis. I feel deep gratitude for him, first of all for getting me involved with extrasolar planets, for the countless hours of discussions, for checking my project and most of all for giving me courage to continue.

To my friends, Kostas Karpouzas, Aggelos Tsiaras, Panagiotis Ioannidis and all the others (you know who you are) thank you for supporting me.

*"http : //home.honolulu.hawaii.edu/ ~ pine/bluedot\_files/bluedot.jpg"*

"That's home," said Sagan.

"That's us..

"Every saint and sinner in the history of our species lived there,  
on a mote of dust,  
suspended on a sunbeam.

"In our obscurity,  
in all this vastness,  
there is no hint that help  
will come from elsewhere  
to save us from ourselves.

"It is up to us."

## Περίληψη

Στο πρώτο μέρος της Πτυχιακής αυτής εργασίας, παρουσιάζουμε την πρώτη στατιστική ανάλυση για αστέρες εξωγαλαξιακής προέλευσης που θα μπορούσαν να φιλοξενήσουν τουλάχιστον ένα εξωπλανήτη. Αναλύουμε τα φωτομετρικά δεδομένα του σφαιροειδή νάνου γαλαξία στη Μικρή Άρκτο (UMi Dwarf), που παρατηρήθηκαν από το τηλεσκόπιο των 2.5 m Isaac Newton Group Telescope (INT) και υπολογίζουμε την πιθανότητα να ανιχνεύσουμε μια διάβαση πλανήτη, με βάση τα χαρακτηριστικά των αστέρων του στατιστικού δείγματος και την κατανομή της πιθανότητας ανίχνευσης με τη μέθοδο των διαβάσεων. Στόχος μας είναι να καθορίσουμε πόσοι πιθανοί πλανήτες θα μπορούσαν να ανιχνευθούν στον γαλαξία UMi Dwarf σύμφωνα με τις μέχρι σήμερα δυνατότητες των τηλεσκοπίων και, ως εκ τούτου, τη δημιουργία του πρώτου καταλόγου με υποψήφιους αστέρες σε έναν άλλο γαλαξία, οι οποίοι θα μπορούσαν να φιλοξενούν πλανήτη, για μελλοντικές διαστημικές αποστολές.

Στο δεύτερο μέρος της Πτυχιακής αυτής εργασίας εφαρμόζουμε μια στατιστική ανάλυση εξωπλανητών στο Γαλαξία μας χρησιμοποιώντας το γαλαξιακό συνθετικό μοντέλο Becanson, για την προσομοίωση της γαλαξιακής και αστρικής κατοικήσιμης ζώνης, προκειμένου να υπολογίσουμε την πιθανότητα ύπαρξης κατοικήσιμων πλανητών. Για να αξιολογήσουμε την κατοικήσιμότητα πλανητών στο Γαλαξία μας, χρησιμοποιήσαμε προσομοιώσεις ποσοστών ( $\alpha$ ) των εκρήξεων υπερκαινοφανών (οι οποίοι συμβάλουν στη δημιουργία νέων αστέρων), ( $\beta$ ) του σχηματισμού πλανητών και ( $\gamma$ ) της κατοικήσιμότητας για μη παλιρροιακά κλειδωμένους πλανήτες. Βρήκαμε ότι το 0,75% των αστέρων στο Γαλαξία μας μπορεί να περιέχει ενδεχομένως κατοικήσιμους πλανήτες.

# Abstract

In the first section of this diploma, we present the first statistical analysis on extra galactic stars that could host an exoplanet. We analyze the photometric data of the Ursa Minor Dwarf (UMi Dwarf) spheroidal galaxy, taken with the 2.5 m Isaac Newton Group Telescope (INT) and we calculate the probability to detect a planetary transit, based on the stellar characteristics of the statistical sample and the transit detection probability distribution. Our goal is to determine how many possible planets could be detected in the above galaxy using today telescope capabilities and therefore to create the first catalogue of extra galactic exoplanet host star candidates for future space missions.

In the second section of this Diploma we apply a statistical analysis of the Milky Way exoplanets using the Becanson galactic synthetic model to simulate the galactic and stellar habitable zones in order to calculate the number of habitable planets. In order to calculate the habitability in our Galaxy, we model supernova rates, planet formation and habitability on non-tidally locked planets. We found that 0.75% of the stars in the Milky Way may possibly contain habitable planets.



# Contents

<b>1</b>	<b>Introduction</b>	<b>9</b>
1.1	Historical Overview . . . . .	9
<b>2</b>	<b>Detection Methods</b>	<b>11</b>
2.1	Radial Velocity . . . . .	11
2.2	Transits . . . . .	13
2.2.1	Transit Theory . . . . .	15
2.3	Gravitational Microlensing . . . . .	19
2.4	Direct Imaging . . . . .	21
2.5	Timing variations . . . . .	21
2.5.1	Pulsar Timing . . . . .	21
2.5.2	Transit Timing Variations . . . . .	22
2.6	Achievements . . . . .	23
<b>3</b>	<b>Discovery probability of extragalactic planets via transit method</b>	<b>25</b>
3.1	Introduction . . . . .	26
3.2	Observational data analysis . . . . .	27
3.3	Probability and Statistics . . . . .	32
3.4	Gaussian noise(white) . . . . .	34
3.5	Noise properties . . . . .	35
3.6	Results . . . . .	39
<b>4</b>	<b>Habitable exoplanets statistics in the Milky Way</b>	<b>41</b>
4.1	Habitable zone . . . . .	42
4.2	Introduction . . . . .	43
4.3	Kepler Statistics . . . . .	43
4.4	Besancon Galactic model . . . . .	44
4.5	Galactic Habitable Zone (GHZ) . . . . .	45
4.6	Stellar Habitable Zone (SHZ) . . . . .	45
4.7	Simulations . . . . .	46
4.8	Results . . . . .	48

8

*CONTENTS*

**5 Conclusions**

**49**

## Σύνοψη

Ξεκινώντας, στο πρώτο κεφάλαιο αυτής της πτυχιακής κάνουμε μια πολύ σύντομη ιστορική αναδρομή περι των φιλοσοφικών αναζητήσεων αλλά και σκέψεων σχετικά με την ύπαρξη άλλης μορφής ζωής πέρα απο τη γη. Απο τα αρχαία χρόνια μέχρι και σήμερα δεν έχουμε απαντήσει στο ερώτημα εαν είμαστε μόνοι σε ολόκληρο το σύμπαν ή όχι. Η πρόοδος της τεχνολογίας και η μεθοδικότητα των επιστημόνων, μας έφερε σε θέση να προσεγγίζουμε ολοένα την απάντηση σε αυτο το ερώτημα με διάφορες άμεσες και έμμεσες τεχνικές.

Κλείνοντας το κεφάλαιο αυτό καταλήγουμε πως έχουμε κάνει αρκετή πρόοδο στο τομέα της αστρονομίας συγκεκριμένα έχοντας συλλέξει πολλά δεδομένα απο διάφορες επιτυχημένες αποστολές, πράγμα το οποίο συνεπάγεται την συνέχεια των ερευνητικών προγραμμάτων, των διαστημικών αποστολών με σκοπό την διεύρυνση των οριζόντων του ανθρώπινου γένους.

Στο δεύτερο κεφάλαιο παρουσιάζουμε τους τρόπους ανίχνευσης πλανητών αναδεικνύοντας τα χαρακτηριστικά του καθενός και τη συνεισφορά τους στην ανακάλυψη νέων εξωηλιακών πλανητών. Αυτοι είναι: (α) με μέτρηση στη μεταβολή της ακτινικής ταχύτητας του αστέρα, (β) με τη μέθοδο των διαβάσεων, (γ) με την παρατήρηση της βαρυτικής μικροεστίασης που προκαλείται από τυχόν πλανήτες που μπορεί να διαθέτει ένα άστρο, (δ) με την άμεση παρατήρηση από τηλεσκόπιο, (ε) με την ανάλυση των χρονικών διακυμάνσεων της περιφοράς ενός πλανήτη γύρω απ' το μητρικό άστρο. Στην παράγραφο σχετικά με τη μέθοδο των διαβάσεων, την αναπτύσουμε περισσότερο απο τις υπόλοιπες παραθέτοντας το μοντέλο διάβασης εξωπλανήτη μπροστά απο αστέρα κατα τον Pàl A. et. al. 2008.

Στο τρίτο κεφάλαιο παρουσιάζουμε τη στατιστική ανάλυση για αστέρες εξωγαλαξιακής προέλευσης που θα μπορούσαν να φιλοξενήσουν τουλάχιστον ένα εξωπλανήτη. Αναλύουμε τα φωτομετρικά δεδομένα του σφαιροειδή νάνου γαλαξία στη Μικρή Άρκτο UMi Dwarf, που παρατηρήθηκαν από το 2.5 m Isaac Newton Group Telescope (INT) με τη χρήση της κάμερας ευρέως πεδίου καθώς και δύο φωτομετρικών φίλτρων με απόκριση στη πράσινη και την ερυθρή περιοχή του φάσματος λευκού φωτός. Προ-

σαρμόζουμε στα δεδομένα μας αστρομετρικό κατάλογο, με σκοπό να μετατρέψουμε τα αστρικά μεγέθη των αστερών του πεδίου μας σε εντάσεις φωτός. Έπειτα κατασκευάζουμε το διάγραμμα χρώματος-μεγέθους αστερών για να βρούμε στατιστικά τα αστέρια που ανήκουν στον εξωγαλαξία. Βρίσκουμε 26 αστέρια στη φασματική περιοχή F0 - G5 και μεγέθους 21.0-24.0 με πιθανότητα να φιλοξενούν πλανήτη. Η πιθανότητα να βρούμε ένα τουλάχιστον πλανήτη στα δεδομένα μας είναι  $58 \pm 4\%$ . Αυτή είναι η ελάχιστη πιθανότητα για τα δεδομένα μας, θεωρώντας πως ένα πολύ μεγαλύτερο τηλεσκόπιο από τα διαθέσιμα τη σημερινή εποχή θα δώσει αρκετά καλύτερα αποτελέσματα, άρα και μεγαλύτερη πιθανότητα να βρούμε ένα τουλάχιστον πλανήτη στα δεδομένα μας. Στη συνέχεια, κάναμε προσομοίωση καμπύλες φωτός με τα χαρακτηριστικά των αστερών που μας ενδιαφέρουν, και είδαμε πως είναι δυνατό να βρεθεί κάποιος πλανήτης εξωγαλαξιακής προέλευσης, μάζας  $M_p = 1M_J$ , ακτίνας  $R_p = 1R_J$  και τυχαίας τιμής περιόδου (1 έως 50 μέρες) με τη χρήση του τηλεσκοπίου των 2.5 μέτρων του INT. Ακόμη, οι προσομοιώσεις με το διαστημικό αστεροσκοπείο - τηλεσκόπιο James Webb Space Telescope (JWST) έδειξαν πως μπορούμε να επιβεβαιώσουμε ένα πλανήτη με τα παραπάνω χαρακτηριστικά, με τη μέθοδο των ακτινικών ταχυτήτων και έχοντας υπόψη ότι για ένα αστέρα φασματικού εύρους F0-G5, και μεγέθους 22 - 24, που φιλοξενεί πλανήτη τύπου hot Jupiter το RMS είναι 1.16 - 3.5 m/sec και εύρος ακτινικών ταχυτήτων 50 - 100 m/sec. Άρα καταλήγουμε στο συμπέρασμα πως είμαστε έτοιμοι να διευρύνουμε τους ορίζοντές μας πέρα απ' το δικό μας Γαλαξία.

Στο τέταρτο και τελευταίο κεφάλαιο της πτυχιακής αυτής εργασίας εφαρμόζουμε μια στατιστική ανάλυση εξωπλανητών στο Γαλαξία μας. Ερευνούμε τον αριθμό των κατοικήσιμων εξωπλανητών. Ως κατοικήσιμη ζώνη ορίζουμε την περιοχή γύρω από ένα άστρο στην οποία ένας γήινης μάζας πλανήτης, με κατάλληλη ατμοσφαιρική πίεση, μπορεί να διατηρήσει νερό σε υγρή μορφή στην επιφάνειά του. Οι πλανήτες που βρίσκονται με τη μέθοδο των διαβάσεων, είναι πολλά υποσχόμενοι στόχοι για το τομέα της αστροβιολογίας αφού μπορεί να μετρηθεί η ατμοσφαιρική τους σύσταση.

Αρχικά, χρησιμοποιούμε τα αποτελέσματα από τους υποψήφιους πλανήτες της διαστημικής αποστολής Kepler, εξαιρώντας όλους τους hot Jupiters ( $2R_E \leq R_p \leq 8R_E$ ), για να βρούμε τη κατανομή της περιόδου των πλανητών. Έπειτα, χρησιμοποιούμε το γαλαξιακό συνθετικό μοντέλο Becanson, για την προσομοίωση των ιδιοτήτων των

αστέρων (Fe/H, mass, distribution). Θεώντας πως ένας κατοικήσιμος πλανήτης καλύπτεται κατά 50% από νέφη  $CO_2$  &  $H_2O$ , υπολογίζουμε την αστρική κατοικήσιμη ζώνη όπως ορίζεται από τον Selsis F. et al. 2007. Οι υπολογισμοί Monte Carlo έδειξαν πως η πιθανότητα απειλής απο σουπερνόβα αυξάνεται δραματικά προς το εσωτερικό του Γαλαξία, και πως ένας κατοικήσιμος πλανήτης δεν μπορεί να σχηματιστεί και να επιβιώσει οπουδήποτε μέσα σε αυτόν. Συμφωνούμε με το σχήμα της κατοικήσιμης ζώνης στο Γαλαξία από τους Gowanlock M. et al. 2011 and Prantzos N. et al. 2008. Χρησιμοποιώντας την υπόθεση πως υπάρχει τουλάχιστον ένας πλανήτης ανα αστέρα (Batalha N. M. et al. 2012), καταλήγουμε στο συμπέρασμα πως υπάρχουν 1.4 δισεκατομμύρια κατοικήσιμοι πλανήτες, ανάμεσα στα 200 δισεκατομμύρια αστέρια στο Γαλαξία μας.



# Chapter 1

## Introduction

### 1.1 Historical Overview

From the ancient years many philosophers thinking about other planets in the universe, in order to figure out if we are alone through all the cosmos. As said greek philosopher Mitrodoros from Chio (~ 4 B.C) : “If someone assumes that the Earth is the only planet with life in the endless universe, in principal he believes, that from one field full of seeds will grow only one of them”. Simplicius of Cilicia cited that the philosopher Anaxagoras (500 B.C) argued that there are infinity number of worlds in the universe. In the following years, many others investigated and believed that there is possibility to exist another habitable planet and maybe life on it, beyond our stellar system. Later Johhannes Kepler discovered the planetary motion laws and at the end of 17<sup>th</sup> century, P. Laplace and E. Kant suggested the first scientific theory for planetary creation. In early 19<sup>th</sup> century, measurments of the temperature of stars, astronomers found out that stars are too hot to harbour life. The German astronomer Otto Struve (Fig. 1.1), was the first person to search for exoplanets examing light curves minimal diminutions due to eclipses (transit method) (Struve O. 1952).

Struve’s believe in the existence of extraterrestrial life and habitable planets because his research on slow-rotating stars, showed him that stars spin at a much lower rate than was predicted by contemporary theories of early stellar evolution, as result of them surrounded by planetary systems which had carried away much of the stars’ original angular momentum, claimed Struve. In 1960, Struve estimated from the big number of slow-spinning stars, there might be as many as 50 billion planets in our Galaxy alone. As he wrote: ”An intrinsically improbable event may become highly probable if the



Figure 1.1: Otto Struve

number of events is very great. ... It is probable that a good many of the billions of planets in the Milky Way support intelligent forms of life. To me this conclusion is of great philosophical interest. I believe that science has reached the point where it is necessary to take into account the action of intelligent beings, in addition to the classical laws of physics.”

Today (Summer 2014) more than 1800 exoplanets have already been discovered. The definition of an extra solar planet is a planet in an orbit around a star different from the Sun. For the discovery of these exoplanets, many teams have used many techniques like radial velocity measurements, photometry (transits), gravitational lensing, astrometry, imaging.

# Chapter 2

## Detection Methods

Compared to its parent star, any planet is an extremely faint light source, furthermore the light from the parent star causes a glare that makes impossible to see the planet. For those reasons, fewer than 5% of the extrasolar planets known as of 2013 have been observed directly. Therefore, astronomers have generally had to resort to indirect methods to detect extrasolar planets. At the present time, several different indirect methods have yielded success.

### 2.1 Radial Velocity

A star with a planet orbiting, will move in its own small orbit in response to the planet's gravity. Because of this influence, there are variations in the speed with which the star moves toward or away from the orbiting planet. The radial velocity(RV) method can be measured from the displacement in the parent star's spectral lines due to the Doppler effect. So the frequency of the light decreases for objects that were receding (redshift) and increases for objects that were approaching (blueshift) as described by the Doppler's law:

$$f = \frac{(c + u_{\star})}{(c + u_{\oplus})} \cdot f_0 \quad (2.1)$$

where  $f$  observed frequency,  $c$  is the speed of light,  $u_{\star}$  the radial velocity component of the star,  $u_{\oplus}$  the relative speed of the observer (Earth) and  $f_0$  is the emitted frequency. The radial velocity of a star can be measured accurately by taking a high-resolution spectrum and comparing the measured wavelengths of known spectral lines to wavelengths from laboratory measurements.

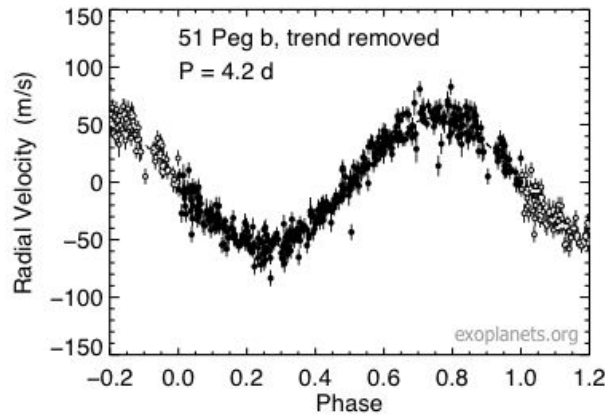


Figure 2.1: The RV diagram of the 51 Peg b. The filled dots are present a full period.

The radial-velocity method measures these variations in order to confirm the presence of the planet. The radius of the star's orbit around the center of mass is so small (due to the greater mass) consequently the velocity of the star around the system's center of mass is much smaller than that of the planet. However, velocity variations down to 0.5 m/s or even somewhat less can be detected with modern spectrometers, (echelle spectrograph at the Keck telescopes). The RV method proved to be the best method for planet hunting because it doesn't depend on the distance, but requires high signal-to-noise ratios to achieve high precision, and so is generally only used for relatively nearby stars out to about 160 light-years from Earth to find lower-mass planets. Even if nowadays spectrographs can easily detect Jupiter-mass planets orbiting 10 astronomical units away from the parent star, the detection of those planets requires many years of observation. Another advantage of the RV method, is that low-mass stars can be detected easier, due to the slower rotation of the main-sequence low-mass stars and so gravitational force of planets is bigger. Spectrum data set is then clearest. In the case of the more massive stars, it is proved to be easy for the detection when the star has left the main sequence, as it slows down the star's rotation. Systems with high inclination to the line of sight of the observer produce smaller wobbles and so they are more difficult to detect. There is also possibility of false signal especially in multi-planet and multi-star systems. Some of these false signals can be eliminated by analyzing the stability of the planetary system.

RV determinations provide estimates of the planetary mass ( $M_p$ ), the eccentricity ( $e$ ) and the semi-major axis ( $a$ ), they do not constrain the inclination ( $i$ ) of the orbital plane with respect to the observer, thus only lower limits to  $M_p$  can be determined. The transit method, on the other hand, provides information on  $i$ , the ratio of the planetary to the stellar radius ( $R_p/R_s$ ), and the duration of the

transit (D). The radial-velocity method can be used to confirm findings made by using the transit method. When both methods are used in combination, then the planet's true mass can be estimated. Although radial-velocity of the star only gives a planet's minimum mass, if the planet's spectral lines can be distinguished from the star's spectral lines then the radial-velocity of the planet itself can be found and this gives the inclination of the planet's orbit and therefore the planet's actual mass can be determined.

## 2.2 Transits

The transit method, provides information on  $i$ , the ratio of the planetary to the stellar radius ( $R_p/R_s$ ), and the duration of the transit (D). It is the second most successful method for extrasolar planets detection. As a planet passes in front of its parent star disk, the observed visual luminosity of the star drops by a small amount. The amount the star dims depends on the relative sizes of the star and the planet.

$$\frac{L}{L_{st}} = \frac{R_p}{R_{st}}^{1/2} \quad (2.2)$$

As mentioned before, transit method determinates the planet radius, and in combination with radial velocity measurements we can compute the real planetary mass and therefore the density. Furthermore, during the transit, the starlight is absorbed passing through the planets atmosphere and so by spectroscopic methods we can figure out the composition of the the planet atmosphere (Charbonneau D. et al., 2002).

Modulation of the combined light of the system during secondary eclipse (the pass of the planet behind the star) provides a direct detection of the planets emergent spectrum focused on the infrared(IR) spectrum region, due to the planet's radiation peak are in the infrared (Deming D. et al., 2005).

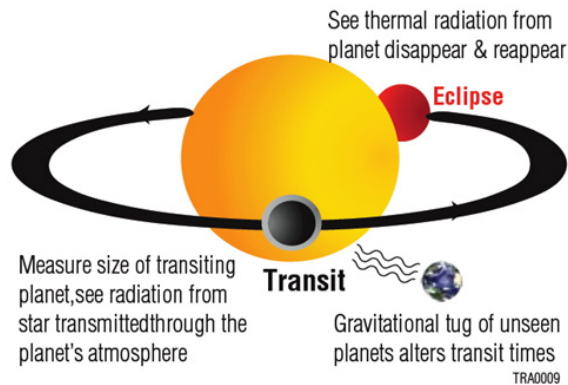


Figure 2.2: Transit and eclipse geometry for a transiting planet. During transit, light from the star is transmitted through the planet's atmosphere. During eclipse, the planet's emitted spectrum is modulated by the eclipse, and is detected via that modulation.

It is possible to explore the atmospheric composition of the planet by the different geometries of transit and secondary eclipse: transit spectroscopy investigate the atmospheric condition between the day and night hemispheres of a tidally-locked planet, whereas secondary eclipse measurements probe the emergent spectrum of the dayside (Knutson H. A. et al. 2008).

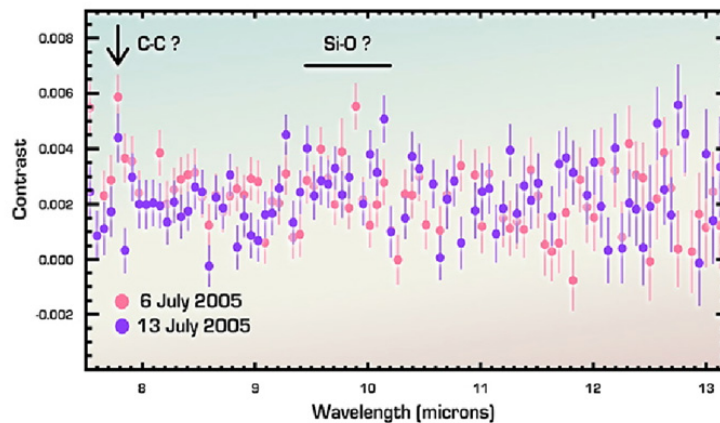


Figure 2.3: Emitted spectrum of the exoplanet HD 209458b, from Spitzer eclipse observations

During transit event one can measure the combined light of star and planet at

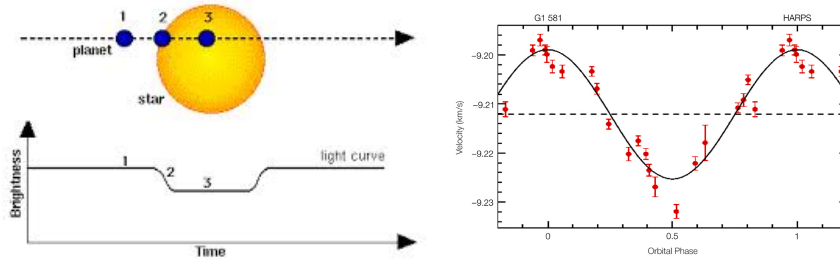


Figure 2.4: **Left:** Transit light curve. **Right** Radial Velocity curve

a large range of orbital phases. Even in tidally locked planets, we can measure the distribution of emergent intensity versus longitude on the planet. Also, the techniques used for transiting systems can also be extended to non-transiting systems, so it is valuable to consider a generalization of the transit technique, namely exoplanet characterization in combined light. Without a transit event, the planet radius cannot be measured directly. Nevertheless, much can be learned, for example from observing fluctuations in IR intensity that are phased to the planets known radial velocity orbit (Harrington J. et al. 2006).

### 2.2.1 Transit Theory

As we said, in the transit event the planet passes in front of the host star and the observer, then the star's observed light dims very little because some amount of the light is blocked by the planet that is much smaller than the star. Each light curve (lc) is like fingerprint, for different planetary system there is different light curve. The light curve inform us about physical characteristics like period, radius of the star-planet, inclination of the planet's orbit etc. Fig. 2.4 shows the geometry of the transit, the transit light curve and the radial velocity curve. Parameters we can measure right away from a lc are, the orbital period of the planet ( $P$ ) because transit is a periodic phenomenon, the depth of the light curve ( $\Delta Flux$ ) and also the duration of the transit ( $D$ ). In case we find interesting results and probably a planet, following up with RV technique could measure the semi-major axis ( $a$ ) and planetary mass ( $M_p$ ) using the equation 2.3 (Charbonneau et al. 2006):

$$K = \left( \frac{2\pi G}{P} \right)^{1/3} \frac{M_p \sin i}{M_*^{2/3}} \frac{1}{\sqrt{1 - e^2}}, \quad (2.3)$$

where  $K$  is the amplitude of the RV curve,  $P$  is the period,  $M_p$  and  $M_*$  is the mass of planet and the mass of the star respectively and  $e$  is the eccentricity of the orbit. The first term of th Eq. 2.3 is function of the semi-major axis  $a$  (Kepler's 3<sup>rd</sup> law).

Supposing we know the mass of the planet ( $M_p$ ) and the semi-major axis of the orbit ( $\alpha$ ) from radial velocity and the duration ( $D$ ), the orbital period ( $P$ ) and the depth of the light curve  $\Delta Flux$  from the transit, using Eq. 2.4 we can derive the radius of the planet ( $R_p$ ) (Seager S., Mallen-Ornelas G. 2003) :

$$R_p = R_s \cdot \sqrt{\Delta Flux} \quad (2.4)$$

and from Eq. 2.5 we can derive the period ( $P$ ), function of duration ( $D$ ), semi-major axis ( $\alpha$ ), the inclination of the orbit ( $i$ ), the radius of the planet and the radius of the star, ( $R_p$ ) and ( $R_*$ ) respectively (Charbonneau D. et al. 2006):

$$D = \frac{P}{\pi} \arcsin \left[ \frac{R_*}{\alpha \sin i} \sqrt{\left(1 + \frac{R_p}{R_*}\right)^2 - \left(\frac{\alpha \cos i}{R_*}\right)^2} \right], \quad (2.5)$$

Continuing, the following basic transit equation is the limb-darkening law. Knowing that the surface of a star does not irradiates homogeneously, as a result the transiting planet does not cover the same amount light, from of the stellar surface. This phenomenon is also known as limb-darkening of transits (Eq. 2.8).

The geometry and the inclination of the system star-planet is crucial for the probability to observe the transit, which proves to be very small. Only if the inclination of the planet's orbit is high enough, we could detect the transit from the Earth. The shortest orbital distance from their host star the bigger the probability. For example, Hot Jupiters this probability is higher because the orbital distance from their host star is smaller. The probability equation for Hot Jupiters detection is

$$P_r = 0.238 \left( \frac{M_*}{M_o} \right) \left( \frac{R_*}{R_o} \right) \left( \frac{P}{d} \right), \quad (2.6)$$

(Gilliland R. L. et al. 2000) where  $M_*$  and  $R_*$  are the stellar mass and radius respectively in solar units and  $P$  is the period of the planet in days. For Eq. 2.6, we assume circular orbits (Hot Jupiters mostly). For larger orbital distances (possible eccentric) we are using a different equation (Seagroves S. et al. 2003)

$$P_r = 0.0045 \frac{1AU}{\alpha} \frac{R_*}{R_o} \frac{1 + e \cos(\pi/2 - \omega)}{1 - e^2}, \quad (2.7)$$

where  $\alpha$  is the semi-major axis,  $e$  is the eccentricity and  $\omega$  is the periastron of the orbit.

### Transit Modeling

Transit light curve data analysis include modeling of the light curve. As a transit model we assume the theoretical light curve of the transit without any noise in our

data. Mandel K. & Algol E. et. al. 2002 or Pál A. et. al. 2008 has work on this field. Below are the basic equation for the Pál's transit model .

We are using a quadratic limb darkening law:

$$I(r) = 1 - \sum_{m=1,2} \gamma_m (1 - \sqrt{1 - r^2})^m, \quad (2.8)$$

where  $r$  is the normalized distance from the center of the star ( $0 \leq r \leq 1$ ),  $\gamma_1$  and  $\gamma_2$  are the limb darkening coefficient (or  $u_1$  and  $u_2$ ) and the flux of the star is

$$f = 1 - \Delta f, \quad (2.9)$$

$\Delta f$  is defined as

$$\Delta f = W_o F_o + W_2 F_2 + W_1 [F_1 + F_K K(k) + F_E E(k) + F_{\Pi} \Pi(n, k)], \quad (2.10)$$

where

$$W_o = \frac{6 - 6\gamma_1 - 12\gamma_2}{6 - 2\gamma_1 - \gamma_2}, \quad (2.11)$$

$$W_1 = \frac{6\gamma_1 + 12\gamma_2}{6 - 2\gamma_1 - \gamma_2}, \quad (2.12)$$

$$W_2 = \frac{6\gamma_2}{6 - 2\gamma_1 - \gamma_2} \quad (2.13)$$

The terms  $F_o$ ,  $F_1$ ,  $F_K$ ,  $F_E$ ,  $F$  and  $F_2$  are only functions of the occultation geometry and the functions  $K(k)$ ,  $E(k)$  and  $\Pi(n, k)$  denote the complete elliptic integrals of the first, second and third kind respectively ( $k$  and  $n$  are constants).

$$K(k) = \int_0^{\frac{\pi}{2}} \frac{d\theta}{\sqrt{1 - k^2 \sin^2 \theta}}, \quad (2.14)$$

$$E(k) = \int_0^{\frac{\pi}{2}} \sqrt{1 - k^2 \sin^2 \theta} d\theta, \quad (2.15)$$

$$\Pi(n, k) = \int_0^{\frac{\pi}{2}} \frac{d\theta}{(1 - n \sin^2 \theta) \sqrt{1 - k^2 \sin^2 \theta}}, \quad (2.16)$$

**Transit-RV Advantages and Disadvantages**

Radial velocity (RV) measurements and transit light curve (LC) analyses have dominated the study of extrasolar planets so far. Both have advantages and disadvantages. While RV determinations provide estimates of the planetary mass ( $M_p$ ), the eccentricity ( $e$ ) and the semi-major axis ( $a$ ), they do not constrain the inclination ( $i$ ) of the orbital plane with respect to the observer, thus only lower limits to ( $M_p$ ) can be determined. The transit method, on the other hand, provides information on  $i$ , the ratio of the planetary to the stellar radius ( $R_p/R_s$ ) and the duration of the transit ( $D$ ). So far, only a combination of both strategies yields a full set of orbital and physical parameters for extrasolar planets.

## 2.3 Gravitational Microlensing

Another method of detecting exoplanets is Gravitational microlensing. This method takes advantage of the gravitational lens effect. When there are random alignments between background source stars and foreground stars which may host planets, background source stars are acting as sources of light that are used to probe the gravitational field of the foreground stars. The relative motion of the source star and lens system allows the light rays from the source to sample different paths through the gravitational field of the foreground system. If there are planets around the lens stars they are changing total gravitational lens magnification of the source star.

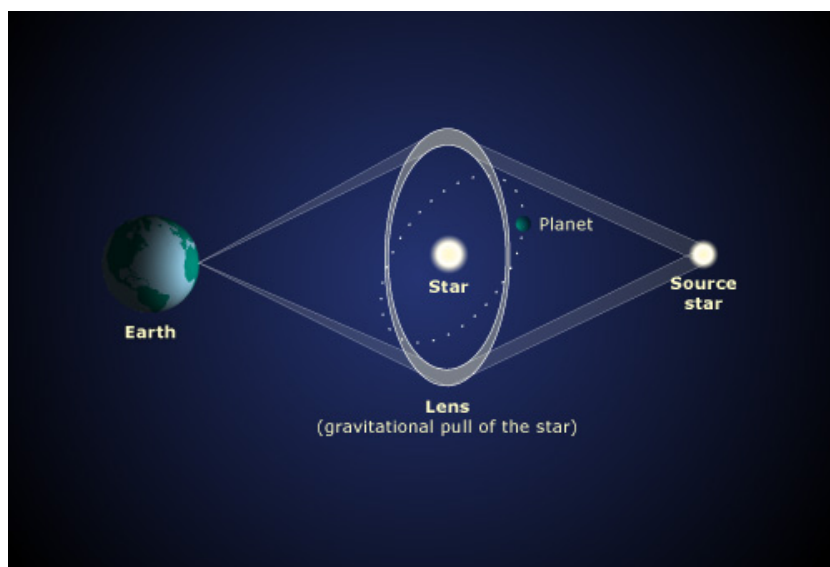


Figure 2.5: Gravitational microlensing of an extrasolar planet

Strong gravitational lensing can be divided into three groups, depending on the lensing object: (1) multiple-images by galaxies, (2) microlensing by stars and giant arcs and (3) large-separation lenses by clusters of galaxies. If the lensing object is a stellar-mass compact object, the image splitting is often too small to be resolved by ground-based telescopes, thus we can only observe the magnification change as a function of time. So, microlensing can be used to detect objects ranging from

the mass of a planet to the mass of a star, regardless of the light they emit, allowing us to study objects that emit little or no light.

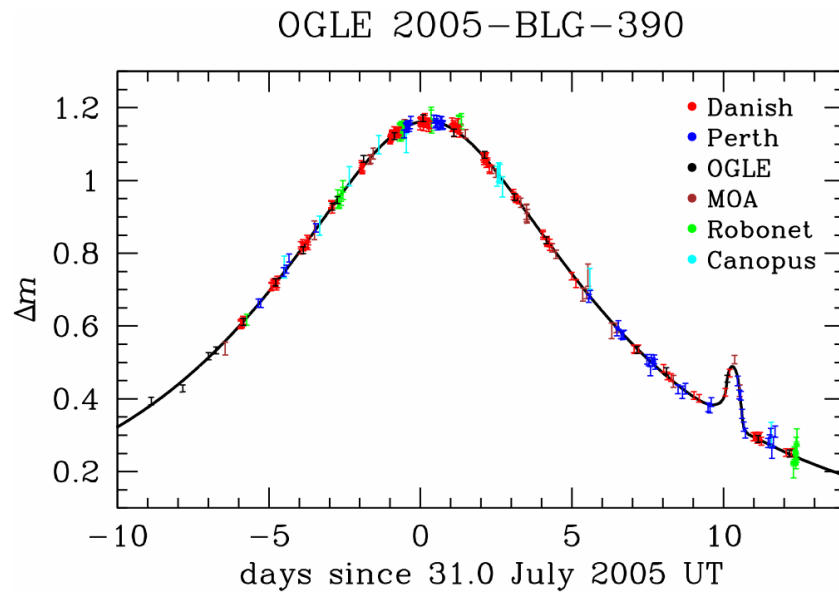


Figure 2.6: Model light curve and data (colour-coded) from 6 different observing sites for the microlensing event OGLE-2005-BLG-390, whose lens star hosts the 5-Earth-mass planet OGLE-2005-BLG-390Lb. The planet revealed its existence by causing a blip of roughly 20% amplitude, lasting about a day, on and around 10 August 2005.

## 2.4 Direct Imaging

The direct imaging of exoplanets is a method detecting exoplanets by obtaining an image of them. This method could be useful on massive planets where orbital distances are much larger than the orbital distance of Neptune. By direct imaging one can obtain luminosity, as well as detailed spectroscopic information. Spectroscopic information can reveal the planets atmospheric chemical compositions. The big disadvantage is that planets are extremely faint light sources compared to stars and the light from them could be lost in the glare of their parent star. So in general, it is very difficult to detect and resolve them directly from their host star.

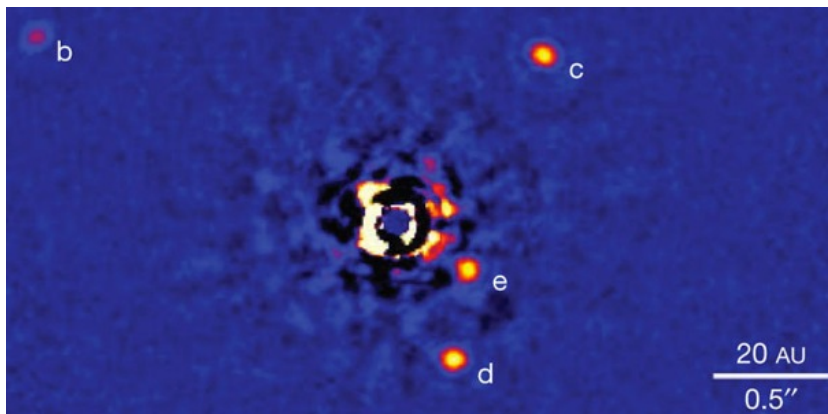


Figure 2.7: HR8799 direct imaging planet detections Credit: Marois et al (2010)

## 2.5 Timing variations

Timing variations on durations of periodic phenomena could be indication of an orbiting planet causing these perturbations on stars or other planets hosting them.

### 2.5.1 Pulsar Timing

A pulsar is a state of star, compact and highly magnetized, neutron star rotating very fast that emits a beam of electromagnetic radiation. Electromagnetic radiation can only be visible when the beam of emission is pointing toward the Earth, like a lighthouse that only be visible when the light is pointed in the direction of

the observer, and periodicity of rotation is responsible for the pulsed appearance of emission. The intrinsic rotation of a pulsar is so precise that slight perturbations in the timing of its observed radio pulses can be used to track the pulsar's motion. In case of orbiting planet, pulsar will move in its own small orbit. Calculations based on pulse-timing observations can reveal the parameters of that orbit. This method is capable of detecting planets far smaller than any other method can, down to less than a tenth the mass of Earth and also detect mutual gravitational perturbations between the various members of a planetary system revealing further information about those planets and their orbital parameters. This method has two main drawbacks: very special circumstances are required for a pulsar planet to form and pulsars are relatively rare. So, this isn't a desired method, because it is unlikely that a large number of planets will be found this way. Also, due to the extreme high-energy radiation near pulsars, life as we know it could not survive on planets orbiting them. Aleksander Wolszczan and Dale Frail (1992) used this method to discover planets around the pulsar PSR 1257+12. This was the first planet outside our Solar System confirmed.

### 2.5.2 Transit Timing Variations

Another method for detecting exoplanets is the method of Transit Timing Variations (TTV). The method is based on how early or late each transit occurs. TTV considered extremely sensitive method capable of detecting additional planets in the system with very small masses. Unidentified planets in the system affect with their gravity the motion of the other bodies on the system, resulting irregularities in their orbital period. For example, calculations and observed data difference of the planet Uranus orbit, resulted to discover planet Neptune in 1846 precisely where supposed to be.

Using the technologically advanced telescopes data (CoRoT, KEPLER), nowadays available, it is easy to confirm the existence of an extra component in a planetary system. Consider we have many accurately timed planetary transits, producing the O-C (observed-calculated) diagram and if there are more than two components in the system the middle epoch of every transit will move around forming a sinusoidal curve.

Using Kepler data, non-transiting planet Kepler-9d was discovered with transit-timing variations method. The transiting planet Kepler-19b shown transit-timing variation with an amplitude of 5 minutes and a period of about 300 days, indicating the presence of a second planet.

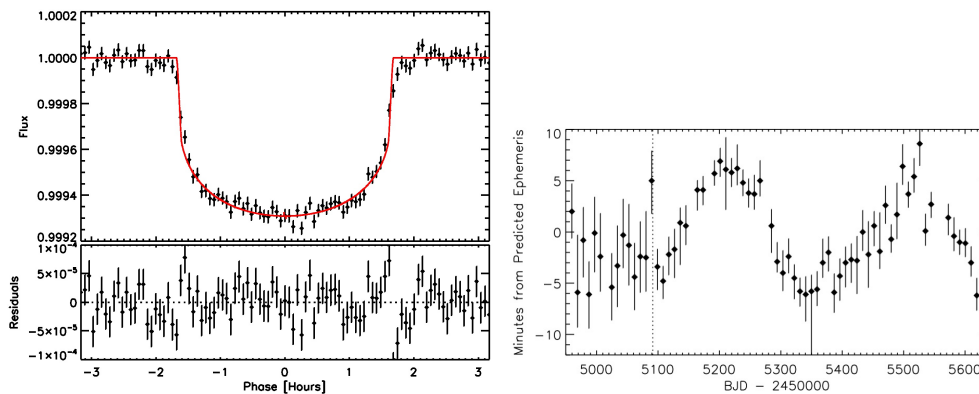


Figure 2.8: **Left:** the folded light curve of KOI 84, after fitting a model to the light curve [up], residuals [bottom]. **Right:** The difference between the predicted and actual times of transit for Kepler-19b. Sometimes, the planet transits 5 minutes earlier than expected and sometimes 5 minutes later. Ballard et al. argue that these transit timing variations are caused by the gravitational influence of a second planet. (fig from the paper)

## 2.6 Achievements

Many planets have been found in the Milky Way by the transit method so far. Hundreds of thousands of stars are monitored, resulting to discover thousands of planet candidates, whose RV follow-up will take many years (and may never be completed for the faintest candidates). Without RV follow-up, the most fundamental parameter of an extrasolar planet, its mass, remains undetermined. The mass is the crucial parameter classifying an object as a planet, brown dwarf or a star. High-accuracy photometry has already been used for a number of systems to show that the planetary thermal emission, as well as the reflection of the stellar light from the planet, are detectable. There were many space and ground survey missions, hunting for exoplanets (Kepler, CoRoT, Qatar) with success, monitoring huge amount of stars in the Milky Way.

Space telescopes CoRoT launched in 2006 (Deleuil et al. 1997) and Kepler launched in 2009 (Borucki et al. 1997), have overcome the atmosphere restrictions thus implement many statistical studies in exoplanets resulting finding many more planets and understanding better the exoplanet characteristics. With the progress of technology and the evolution of telescopes, new space telescope missions have gotten approval PLATO, TESS, EChO (waiting) (Tinetti G. et al. 2012) and James Web observatory (replacing Hubble) would make statistical studies better.



## Chapter 3

# Discovery probability of extragalactic planets via transit method

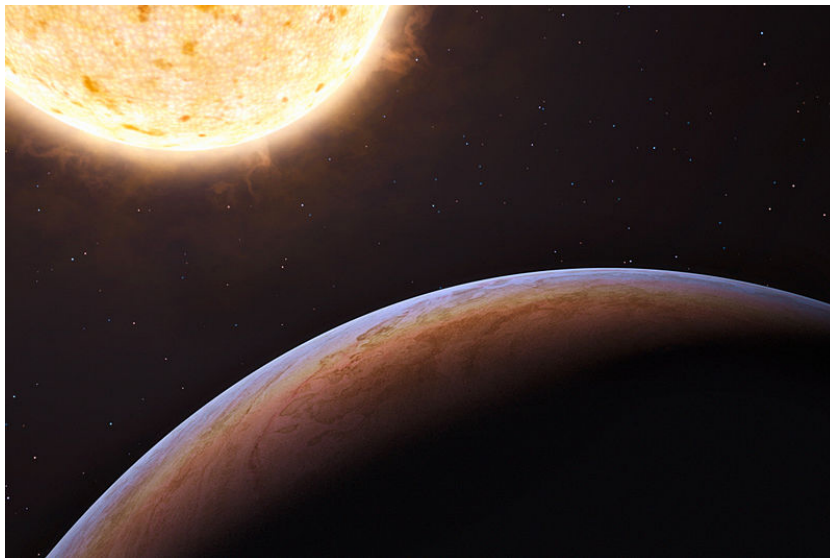


Figure 3.1: Artist's impression of HIP 13044b, the first discovered planet of extragalactic origin.

In this section we estimate the possibility to find an exoplanet with extragalactic origin, regarding today's telescope capabilities and the instrumentation provided in general, in order to figure out if we can detect a planet with extragalactic origin. Such a discovery would increase our knowledge for exoplanets and would be a step further for our existential questions.

### 3.1 Introduction

Many planets have been found in the Milky Way by the transit method so far. There were many space and ground survey missions, hunting for exoplanets (Kepler, CoRoT, Qatar) with success, monitoring huge amount of stars in the Milky Way. Space telescopes Kepler (Borucki W. et al. 1997), CoRoT (Deleuil et



Figure 3.2: Kepler telescope

al. 1997), have overcome the atmosphere restrictions thus implement many statistical studies in exoplanets resulting finding many more planets and understanding better the exoplanet characteristics. With the progress of technology and the evolution of telescopes, new space telescopes PLATO, TESS<sup>1</sup> would make statistical studies better.

In this diploma we use the statistics already applied in our galaxy. Baltz E. A. & Gondolo P. 1999 make reference to extragalactic planets, looking for gravitational microlensing events of unresolved stars. Furthermore Setiawan J. et al. 2010 made reference for detection of an extragalactic planet, but eventually Jones M. I. & Jenkins J. S. 2014, showed that there isn't any planet near HIP13044 star, which has been connected to the Helmi stream (Helmi A. et al. 1999), a group of stars that share similar orbital parameters that stand apart from those of the bulk of other stars in the solar neighborhood.

---

<sup>1</sup><http://tess.gsfc.nasa.gov/>

## 3.2 Observational data analysis

In order to estimate the probability to discover an extragalactic planet, we make use of the 2.5m Isaac Newton of Telescope (INT) public data archive and the Cambridge Astronomical Survey Unit<sup>2</sup>. The target was Ursa Minor Dwarf elliptical galaxy (RA=15:08:24, Dec=+67:25:00)  $60 \pm 10$  kpc (Gilliland R. et al. 2000) away, with apparent magnitude 11.9 (NASA/IPAC Extragalactic Database). The Ursa Minor dSph galaxy was observed with the INT WFC on 2000 July 6 through the 214 ( $\sim R$ ) and 220 ( $\sim G$ ) Sloan photometric filters, and the exposure time was 600 seconds. The WFC aperture was centered on the target position. One fast readout observation were obtained in each filter (table 3.1). The Wide Field Camera (WFC) is an optical mosaic camera for use at the prime focus of the 2.5m Isaac Newton Telescope (INT). The WFC consists of 4 thinned EEV 2kx4k CCDs. The CCDs have a pixel size of 13.5 microns corresponding to 0.33 arcsec/pixel. The edge to edge limit of the mosaic, neglecting the ( $\sim 1$ ) arcmin inter-chip spacing, is 34.2 arcmins. The cycle time for the whole mosaic is around 42 seconds. A maximum of 6 filters could be installed in the wheel. Both broadband and Stromgren filter sets are available, as well as a range of narrowband filters. Operating temperature is -153K. In table 3.2 and fig. 3.3 we see Quantum Efficiency of each CCD and EEV4280 (detector) respectively.

CCD	Noise (e)	Noise (ADU)	Gain (e/ADU)	Bias
1	9	3.6	2.5	1830
2	9.5	2.8	3.4	1810
3	7.7	3.2	2.4	1835
4	9.1	2.8	3.25	1810

Table 3.1: WFC-CCDs Operational Characteristics-FAST readout 29 seconds

Wavelength	380nm	400nm	650nm	950nm
CCD1	67	80	75	13
CCD2	72	87	79	15
CCD3	62	80	80	14
CCD4	61	78	86	16

Table 3.2: Quantum Efficiency (-120C)

---

<sup>2</sup>[www.casu.ast.cam.ac.uk](http://www.casu.ast.cam.ac.uk)

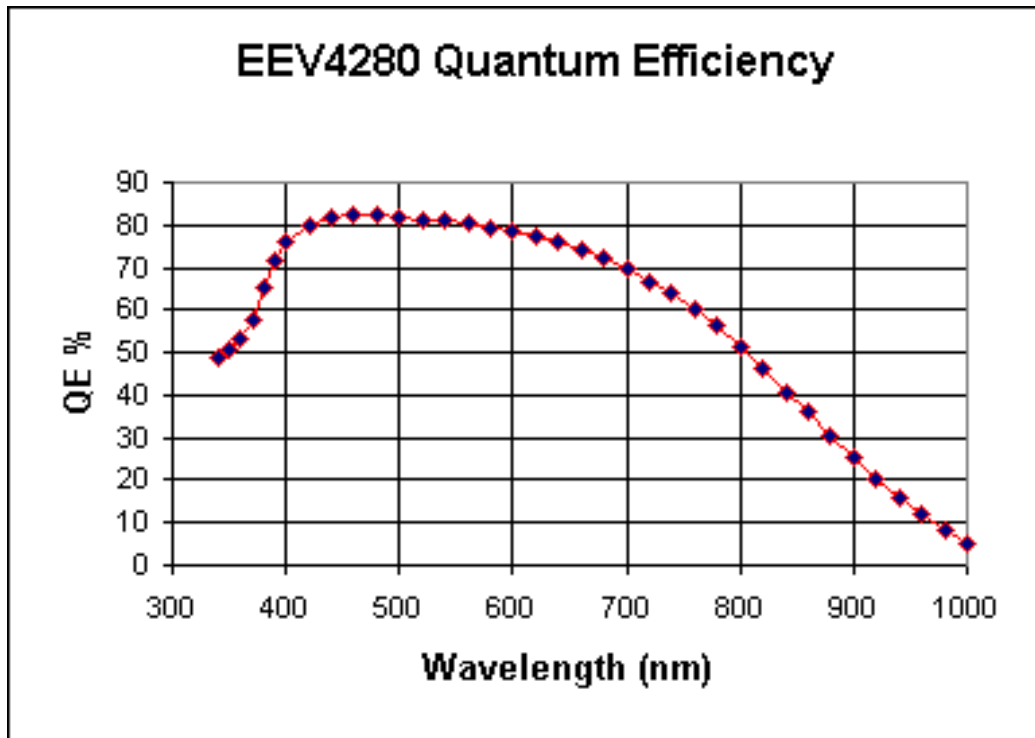


Figure 3.3: Full QE curve for EEV4280 in tabulated measured at ATC March 99

These INT observations indicate that Ursa Minor has had a very simple star formation history consisting mainly of a single major burst of star formation about 14 Gyr ago which lasted  $< 2$  Gyr, and clearly show that most of the stars in the central region of the galaxy are ancient, probably as old as the Milky Way (Mighell K. J. & Burke Ch. J. 1999).

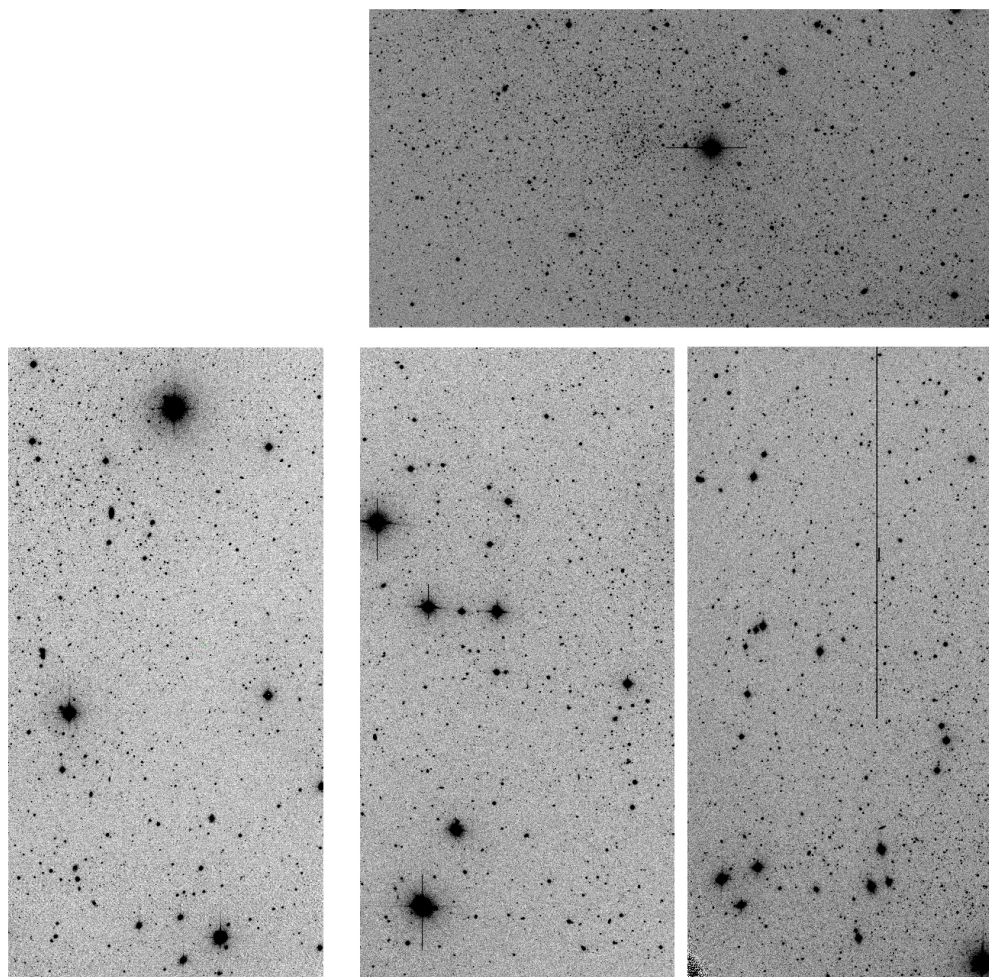


Figure 3.4: Negative mosaic image of the WFS09 data set, Ursa Minor Dwarf spheroidal galaxy field

For the photometry and the astrometry we used Starlink/Extractor software (Draper P. W. et al. 2014). Extractor is a program for automatically detecting objects on an astronomical image and building a catalogue of their properties. It is particularly suited for the reduction of large scale galaxy-survey data, but also performs well on other astronomical images.

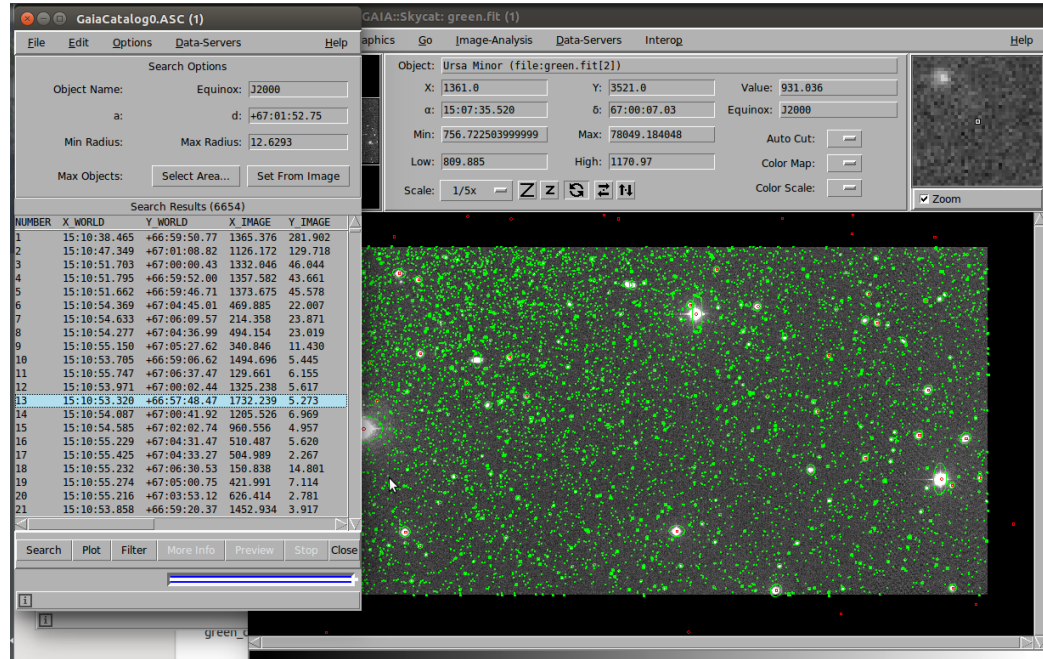


Figure 3.5: Performing GAIA: Starlink/Extractor software

In transit light curve analysis we use the measured flux of the stars to draw conclusions. Thus, we use the magnitude to flux relation is given as follows (eq. 3.1):

$$m_1 - m_2 = -2.5 \cdot \log_{10}(L_2/L_1) \quad (3.1)$$

where  $m_i$ ,  $i=1,2$  is the stellar magnitude and  $L_i$ ,  $i=1,2$  is the luminosity, for stars 1 and 2.

In order to normalize our results of photometry to the real magnitude system in both filters, we fit the UCAC4 catalogue (Zacharias N. et al. 2012). Also, we keep in mind that each CCD has different QE in each filter (table 3.2). Figure 3.6 shows an example of ADU-to-Magnitude cross correlation curves for red and green band.

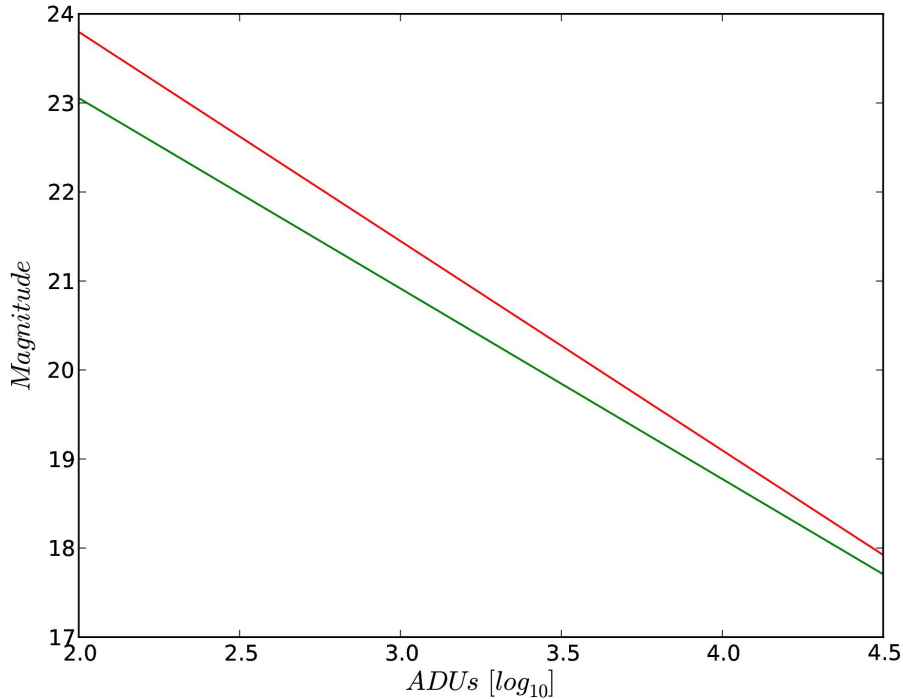


Figure 3.6: ADUs-to-magnitude plots for red (red solid line) and green (green solid line) Sloan Photometric filters respectively.

HertzsprungRussell(HR) diagram is a 2D plot where stars of greater luminosity are toward the top of the diagram, and stars with higher surface temperature are toward the left side of the diagram.

The original HR diagram display the absolute visual magnitude on the vertical axis and the spectral type of stars on the horizontal axis.

Observational astronomers use color-magnitude diagram (CMD), which is a HR diagram where spectral type is replaced by a color index (eg.B-V) of the stars. CMD is a valuable diagram in cases demanding to find foreground and background stars, due to the correlation between distance and extinction. A color-magnitude diagram(CMD) help us to distinguish the stars belonging to Ursa Minor dSph galaxy to those of the Milky Way (foreground and background stars).

Figure 3.7 shows the photometric results as a color-mag diagramm. We can also distinguish the stars belong to Ursa Minor galaxy to those of the Milky Way by the two giant branch from which one belongs to Milky Way (blue) and the other to Ursa Minor galaxy (red).

As we expect, Ursa Minor stars suffer by more absorption due to greater distance. In the distance of 60kpc the magnitude range of main sequence magnitudes (F0-

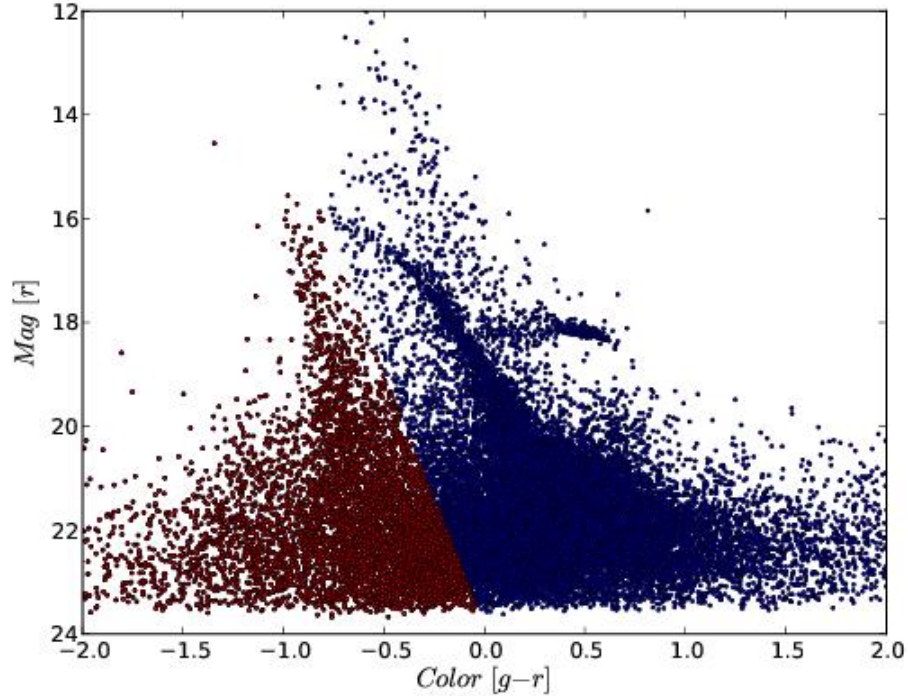


Figure 3.7: Color-Magnitude diagram of Ursa Minor galaxy. The left giant branch belongs to Ursa Minor and the right one to Milky Way.

K8) is 21.89 to 26.89, but we are not able to observe fainter stars than 24<sup>th</sup> with INT. Thus our range true magnitude range is 21.9 to 24.0 (F0-G5 spectra type stars). In this range we have add the absorbtion of  $A_V = 0.09$  (Mighell K. J. & Burke Ch. J. 1999).

The total photometric Catalogue from INT's data contains 30,332 stars which 5969 belongs, statistical, to Ursa Minor Galaxy. Applying the magnitude range (F0-G5 type stars) in the photometric catalogue, we find that there are 2034 stars in that spectral type range.

### 3.3 Probability and Statistics

In this section we calculate the probability and apply statistics in our sample. In order to measure the probability of the existence of a planet harbour a star we refer to Howard A. W. et al. 2012, that shows us the distribution of hot Jupiters with period up to 50 days is 0.013 per star.

After that, we must calculate geometrical transit possibility to actually locate this planet, which depending on the relative position star-planet system.

As we know, planetary transits are only observable for planets whose orbits happen to be perfectly aligned (small inclination) from the astronomers' vantage point. The probability of a planetary orbital plane being directly on the line-of-sight to a star is the ratio of the diameter of the star to the diameter of the orbit. About 10% of planets with small orbits have such alignment, and the fraction decreases for planets with larger orbits.

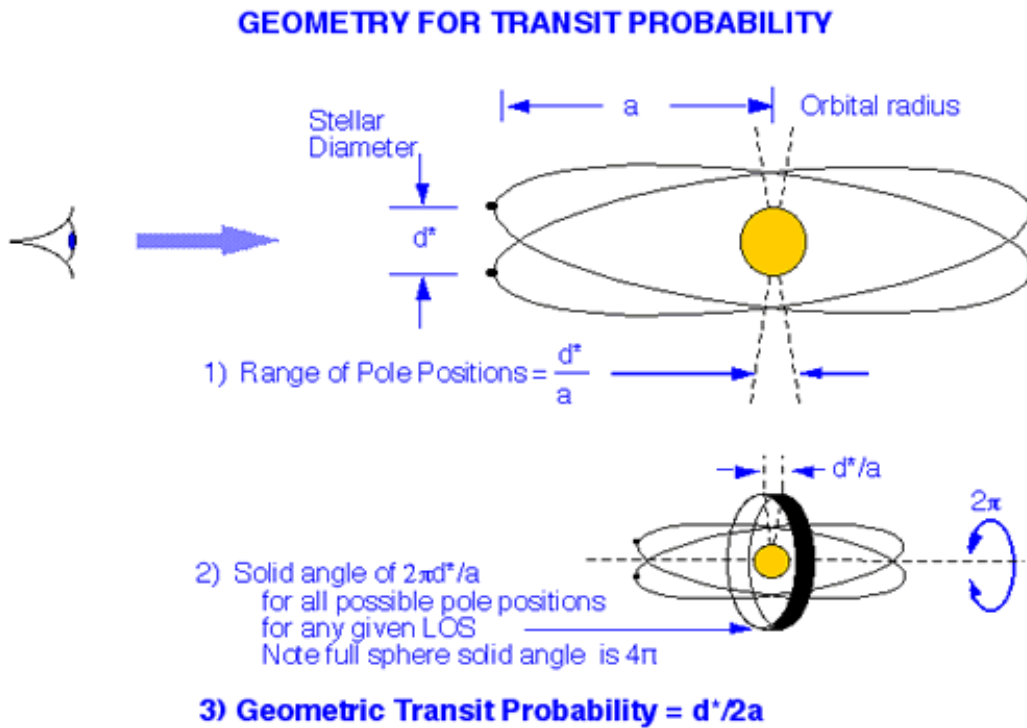


Figure 3.8: Geometry for transit probability

The geometrical transit probability is given by eq. 3.2

$$P_{geo} = 0.238 \cdot M^{-1/3} \cdot R \cdot P^{-2/3} \quad (3.2)$$

where  $M$  and  $R$  are the host star mass and radius in solar masses and solar radii respectively.  $P$  is the period of the planet in days. Applying Howard A. W. et al. 2012 results in our sample we find 26 candidate stars with the probability to host a hot Jupiter. In order to calculate the transit probability we are using Monte Carlo simulations and eq.3.2. After 1000 integrations we find that the probability to discover at least one transit in INT sample is  $58\% \pm 4\%$ . Figure 3.9 shows the probability distribution (58%) and the error (4%), corresponding to  $1\sigma$  of it.

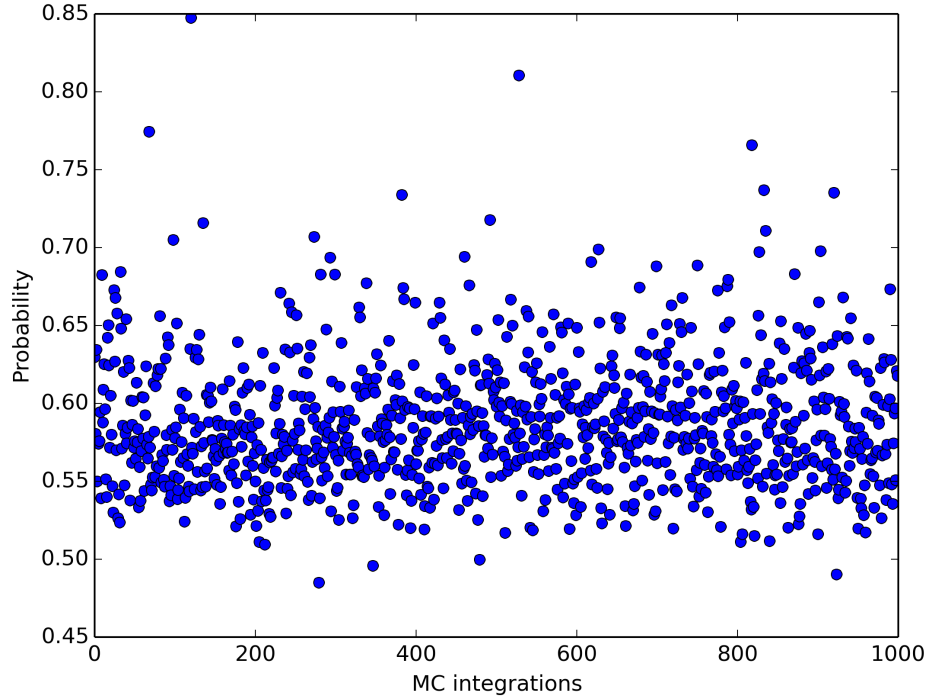


Figure 3.9: Probability distribution.

### 3.4 Gaussian noise(white)

Gaussian noise is statistical noise having a probability density function (PDF) equal to that of the normal distribution, which is also known as the Gaussian distribution. In other words, the values that the noise can take on are Gaussian-distributed.

The probability density function  $p$  of a Gaussian random variable  $z$  is given by eq.3.3:

$$p_G(z) = \frac{1}{\sigma \sqrt{2\pi}} e^{-\frac{(z-\mu)^2}{2\sigma^2}} \quad (3.3)$$

where  $z$  represents the grey level,  $\mu$  the mean value and  $\sigma$  the standard deviation.

### 3.5 Noise properties

Using the exposure calculator for the INT telescope<sup>3</sup>, S/N - Magnitude data fitting resulted in eq. 3.4

$$S/N = 10^{9.5122-0.35 \cdot \text{mag}} \quad (3.4)$$

where S/N is the signal-to-noise ratio for INT. Fig. 3.10 we can see the graph of S/N-Mag for the INT.

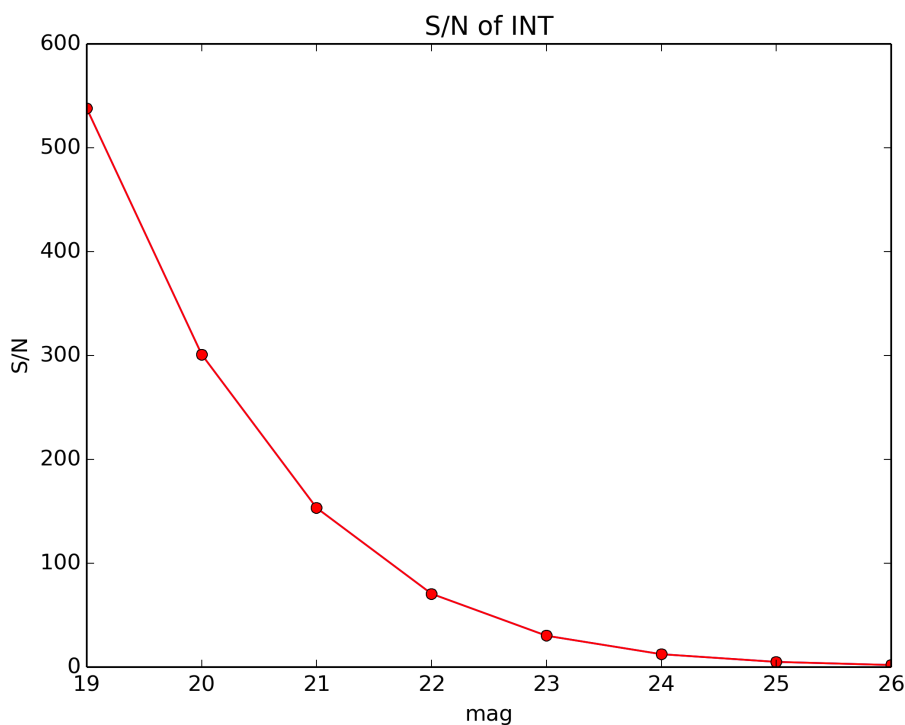


Figure 3.10: S/N- magnitude diagram of INT

According to equation 3.4, we made simulated transit light curves, according Pál 2008 transiting model. For our simulations we assume hot Jupiter with mass  $M_p = 1M_J$ , radius  $R_p = 1R_J$  and random period range 1 to 50 days, according to period distribution for hot Jupiter. The magnitude range for the UMi Dwarf galaxy is 21.0-24.0 (F0 - G5 type stars). Fig. 3.11 shows two sample phase folded light curves with magnitudes 21.0 and 24.0 respectively, periods for 1 and 50 days and spectral types G5 and F0, which is our best and worse scenario. The integration time for both is 1000 seconds.

<sup>3</sup><http://catserver.ing.iac.es/signal>

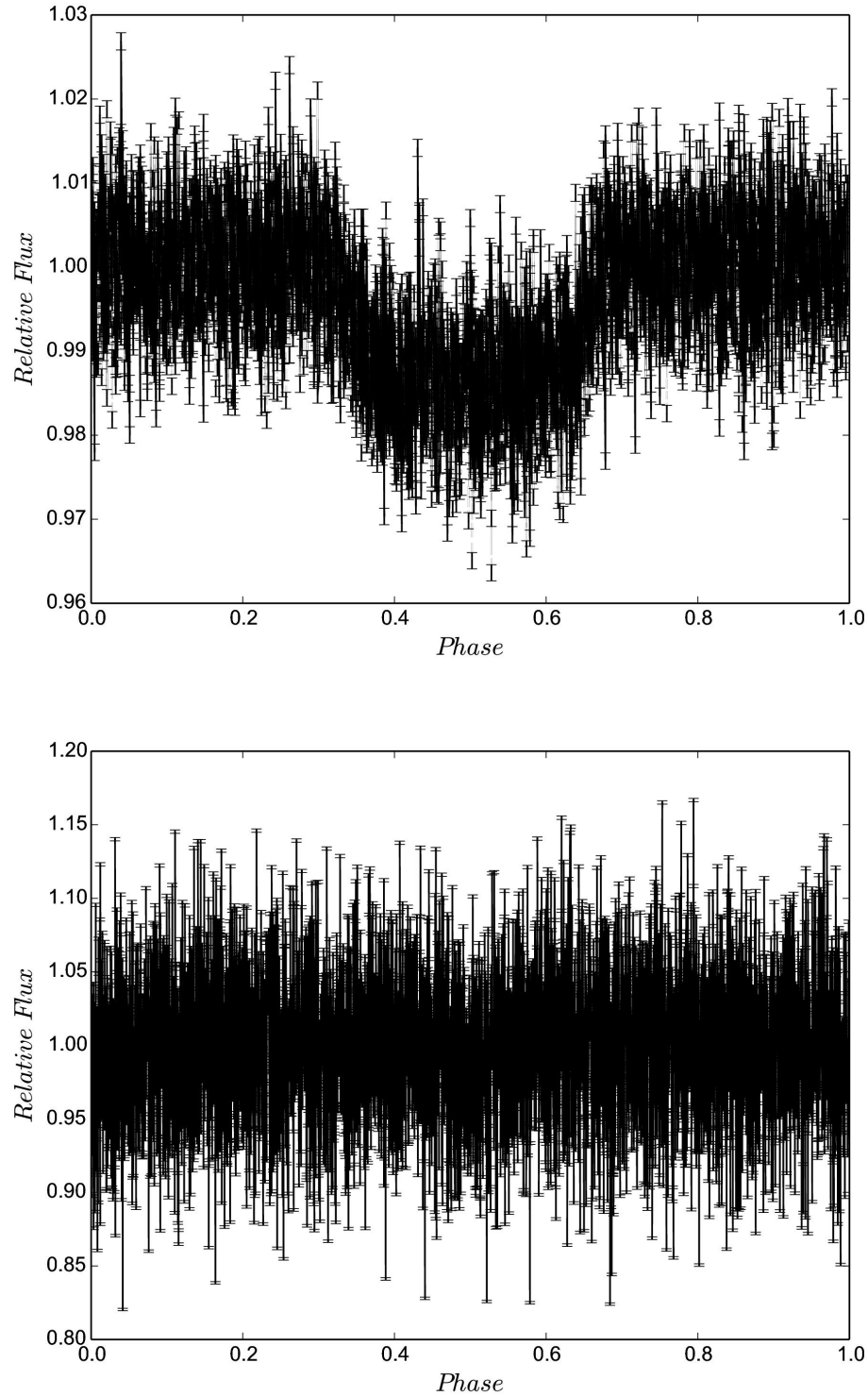


Figure 3.11: Simulated light curve for INT S/N calculator. Spectral type G5 and F0, period 1 to 25 days, magnitude 21.0(top) to 24.0(bottom) respectively. Exposure time 1000 secs.

After that, we make use the exposure calculator for the James Webb Space Telescope (JWT) <sup>4</sup>, in order to figure out if we can use the JWT<sup>5</sup> to confirm an event by radial velocity method also. For a F0-G5 22 mag star the resulted S/N is 85.9 and the RMS is 1.16m/sec. Respectively, for a F0-G5 24 mag star the resulted S/N is 28.3 and the RMS is 3.5m/sec. Considering that a typical hot Jupiter host star has 50 to 100 m/sec radial velocity range, we conclude that we are capable of an radial velocity follow up of an event using the JWT.

Fig. 3.13 shows two sample radial velocity curves 50m/sec peak, with magnitudes 21.0 (S/N 85.9620, RMS 1.16m/sec) and 24.0 (S/N 28.26, RMS 3.5m/sec) respectively (F0-G5).

---

<sup>4</sup><http://jwstetc.stsci.edu/etc/>

<sup>5</sup><http://jwst.nasa.gov/index.html>

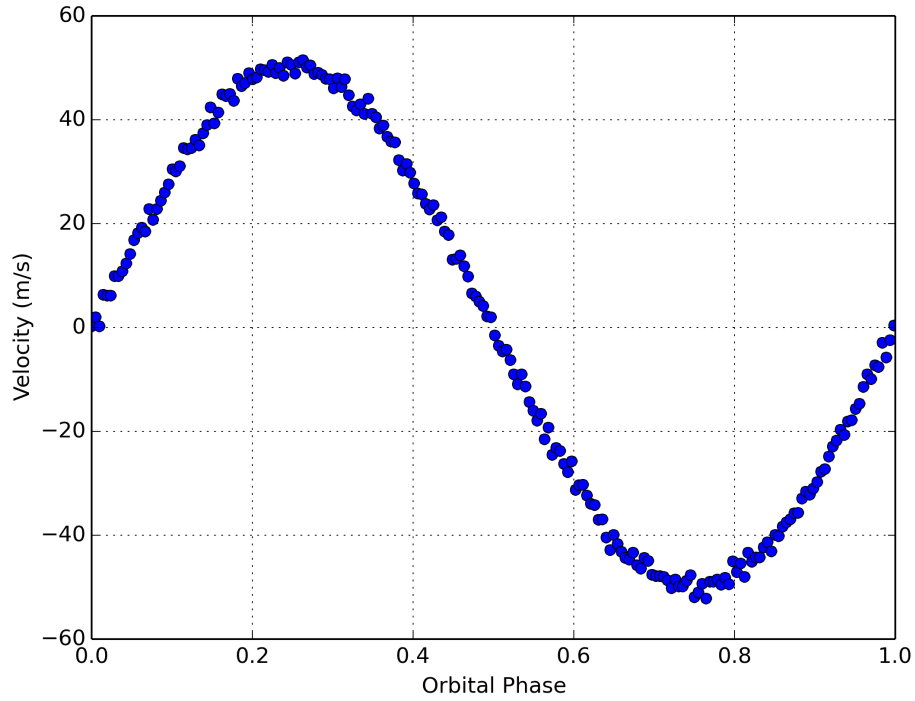


Figure 3.12: Simulated radial velocity curve for a F0-G5 22 mag star, S/N 85.9620 and RMS 1.16m/sec

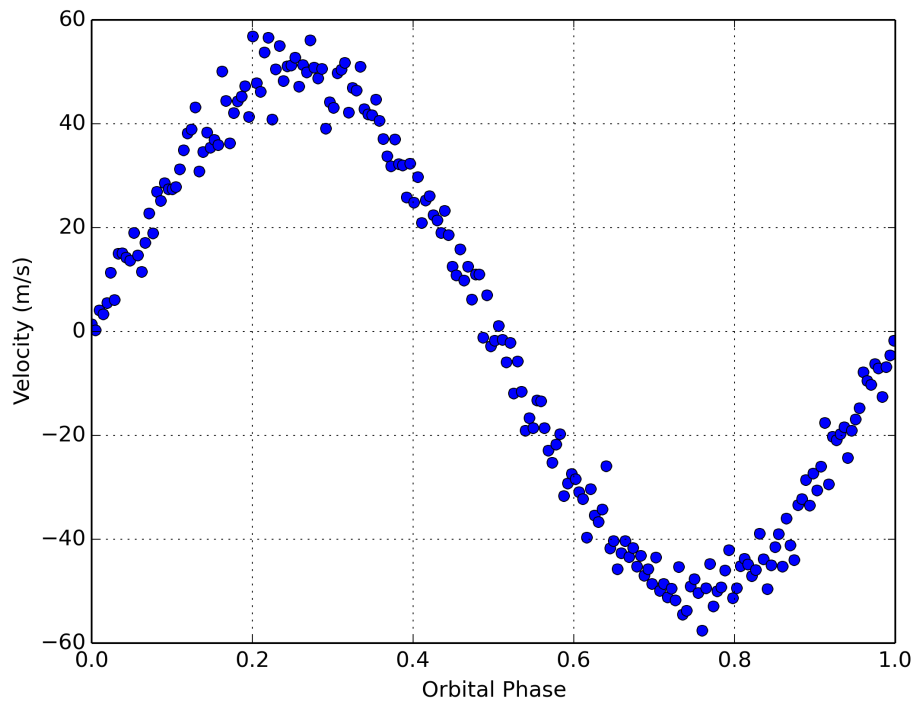


Figure 3.13: Simulated radial velocity curve for a F0-G5 24 mag star, S/N 28.26 and RMS 3.5m/sec

## 3.6 Results

We present a statistical analysis about existence of transiting extragalactic planets in Ursa Minor Dwarf spheroidal galaxy. We find that the probability to discover at least one transit in INT sample is  $58\% \pm 4\%$ . We consider this probability is the minimum of our magnitude range, assuming a bigger telescope gives out much bigger possibility. Considering JWT will be launched in the near future RV follow up won't be a problem at all. So, we conclude that the possibility of finding a transit event like this is efficient nowadays.



## **Chapter 4**

# **Habitable exoplanets statistics in the Milky Way**



## 4.1 Habitable zone

Circumstellar habitable zone (CHZ), or habitable zone (HZ), is the region around a star within which planetary-mass objects with sufficient atmospheric pressure can support liquid water at their surfaces. The shape of the HZ is calculated by the use of planets position in the orbiting star, the amount of the radiant energy it receives from it, and the known requirements of life on Earth's biosphere. The dominant element, searching for extraterrestrial life and intelligence, is the investigation for liquid water.

HZ concept was presented in 1953. From then on many planets have been discovered in the HZ, the majority of them are more massive than Earth, because such planets are easier to detect. Statistical studies excluded from Kepler space mission data imply that there could be as many as 40 billion earth-sized planets orbiting in the habitable zones of sun-like stars and red dwarf stars within the Milky Way. 25% of them may orbit sun-like stars. Furthermore, there are many studies on the emerging field of natural satellite habitability (Kipping D. M. et al. 2012), because planetary-mass moons in the CHZ might outnumber planets.

A visualization of the habitable zone is shown below in fig.4.1. The red region is too warm, the blue region too cool, and the green region is just right for liquid water.

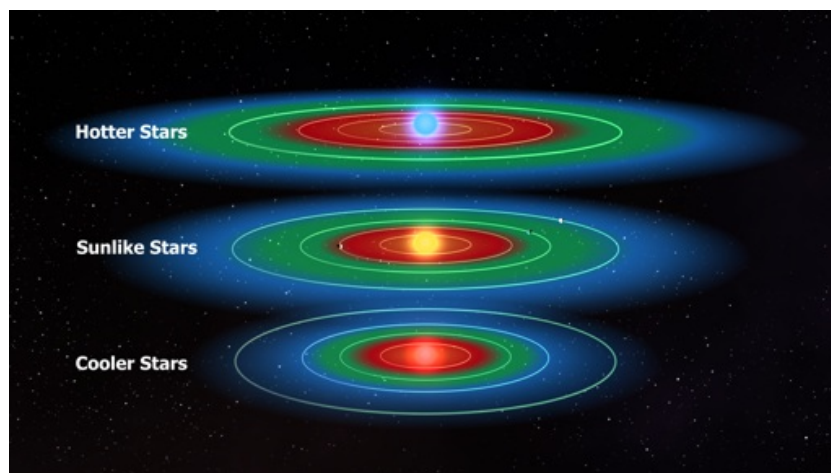


Figure 4.1: Schematic of habitable zone of different planets

In the following years, discovery of evidences of substantial quantities of extraterrestrial life, believed to occur outside the HZ. The necessary components of water-dependent life, may be found even in interstellar space on rogue planets or their moons, support by other energy sources, such as radioactive decay, tidal

heating or pressurized by other non-atmospheric means.

## 4.2 Introduction

Astrobiology flourishes with the help of transiting extrasolar planets data. Those targets advantage is that they offer direct measurements of the atmospheric composition of potentially inhabited worlds with spectrum analysis assist. The recent detections of the transiting Kepler-22b (Borucki W. et al. 2012), as well as observations of the rest, approximately 40 habitable candidates from Kepler, have shown that today's technology is mature for the exploration of terrestrial planets and their habitability.

There are many studies about the Stellar Habitable Zone (SHZ) and the Galactic Habitable Zone (GHZ) since the first exoplanet. The SHZ is more easy to use, because the definition the habitable zone (water in liquid form).

Selsis F. et al. 2007 gave a more sofisticate model of the SHZ. The GHZ, on the other, is much more difficult to define. Today there are some studies about GHZ such as Gonzalez G., Brownlee D. 2001, Lineweaver C. et al. (2004), Prantzos N. et al. 2006 & Gowanlock M. et al. 2011. All these models is a theoretical approximation to the problem. Gonzalez G. & Brownlee D. 2001, Lineweaver C. et al. 2004, for example suggest that the GHZ shape is a ring around the galactic center (similar to the SHZ), and habitable planets, can not formed or survive outside of the zone. Prantzos N. et al. 2006 suggests that the hole Galaxy could be a giant habitable zone, and habitable planets could be anywhere. Our approximation to the problem differs from all the above studies. We are using a synthetic model of the Milky Way (Besancon - Robin A. et al. 2003), in order to simulate 200 billion stars and then to measure the possible habitable planets. Also, we include to our model the Kepler statistical results.

## 4.3 Kepler Statistics

The period distribution for small planets is extremely important but unknown for many years. In order to extract the most reliable one, we are using the results from Kepler candidates excluding all hot Jupiters. The radius threshold we use is  $2R_E \leq R_P \leq 8R_E$ .

The period distribution of the small Keplers candidates, suffers by the geometrical probability trend. The geometrical probability is given by Seagroves S. et al. 2003

$$\Psi_{geo} = 0.238 \cdot M^{-1/3} \cdot R \cdot P^{-2/3} \quad (4.1)$$

where  $M$  and  $R$  are the host star mass and radius in solar masses and solar radii respectively.  $P$  is the period of the planet in days.

After we remove the geometrical probability (Seagroves S. et al 2003) from Kepler candidates, we find the best Gauss fit for the upper & lower error level (Fig. 4.2).

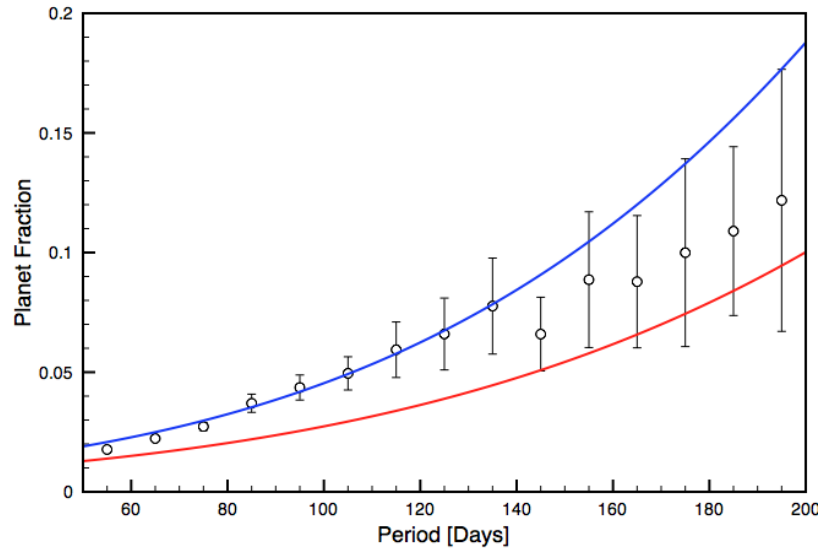


Figure 4.2: Period distribution and upper - lower error limit (Kepler candidates).

It is true that we do not know how the period distribution continues after  $P=1.3$  years, and we need more data.

## 4.4 Besancon Galactic model

In order to simulate the stellar components of the galaxy, we made an extensive use of the Besancon model of the Milky Way (Robin A. et al. 2003), which returns the atmospheric parameters and the distances of simulated stars towards a given line of sight.

This model assumes a galaxy composed by a multiple-ages thin disc, and single ages thick disc, halo and bulge. Since we are only interested in the intrinsic properties of the stars (galactocentric distances,  $T_{\text{eff}}$ ,  $\log g$ ,  $[\text{Fe}/\text{H}]$ ) and not on the observed quantities (magnitudes, radial velocities), the query did not include any extinction, nor limit in the apparent stellar magnitudes.

We took advantage of the symmetries of the model to request only simulations for a quarter of a sphere, and interpolate from this query to the total galaxy. Hence,

our modelled Milky Way has been obtained from the results for  $l=[0,180]$  and  $b=[0,90]$ , which have been normalized to the total Galaxy. In total, our mock Galaxy contains  $2 \times 10^{11}$  stars.

## 4.5 Galactic Habitable Zone (GHZ)

In this study, we do not represent the Galactic Habitable Zone (GHZ), but we are using the results from other studies about GHZ (Gonzalez & Brownlee 2001, Lineweaver et al. 2004, Prantzos et al. 2008, Gowanlock et al. 2011). First we need the stellar characteristics such as spectral type, age, galactic position, luminosity and stellar distribution. As we describe above, we extract all these values from the Besancon model (Robin et al. 2003). According to Gowanlock et al. (2011), type Ia SNe (SNI) and type II SNe (SNII) could affect the habitability of a planet. The affecting distance is given by eq.4.2:

$$d_{SN} = 8 \sqrt{10^{-0.4(M_{abs}+17.505)}} \quad (4.2)$$

where  $d_{SN}$  is the affecting SN sphere radius in pc (Gehrels et al. 2003, Gowanlock et al. 2011) and  $M_{abs}$  is the stellar absolute magnitude. As a SNI and SNII possible sources we assume all the main sequence stars with masses  $M_{\star} \geq 8M_{\odot}$  and the 1% of white dwarfs respectively (Gowanlock et al. 2011). In our model, the minimum stellar age for Ozone reconstruction & complex life time, were set to 4.25 Gyr according to Lineweaver et al. (2004), Prantzos et al. (2008) & Gowanlock et al. (2011).

## 4.6 Stellar Habitable Zone (SHZ)

We are using the Stellar Habitable Zone (SHZ) definition by Selsis F. et al. 2007. Assuming that the habitable planet is covered 50% by clouds (CO<sub>2</sub> and H<sub>2</sub>O), the equation for the limits of the habitable zone are given by eq.4.3:

$$d_{in,out} = (c_{in,out} - a_{in,out}T_D - b_{in,out}T_D^2) \left( \frac{L_{\star}}{L_{\odot}} \right)^{0.5} \quad (4.3)$$

where  $c_{in,out} = 0.895$  and  $1.25$ ,  $a_{in,out} = 2.7619 \cdot 10^{-5}$  and  $1.3786 \cdot 10^{-4}$ , and  $b_{in,out} = 3.8095 \cdot 10^{-9}$  and  $1.4286 \cdot 10^{-9}$ , for the inner and outer habitable zone limits respectively. Also,  $L_{\star}$  is the stellar luminosity and  $T_D = T_{\star} - T_{\odot}$ .

## 4.7 Simulations

Monte Carlo simulations shows, that a SN threat probability increases dramatically for the inner part of the Milky Way. Thus, we agree with Gowanlock M. et al. 2011 and Prantzos N. et al. 2008, about the shape of the Galactic Habitable Zone (GHZ). Our simulations have shown, that a habitable planet can not be formed and survive everywhere in the Galaxy. In contrast, Gonzalez G. & Brownlee D. 2001, Lineweaver C. et al. 2004 suggested a ring-shape of the GHZ, but we have no evidence to support this theory.

Using the stellar main sequence and white dwarf stars distribution by the Besancon model, we calculate the SN contribution for the formation of the habitable planets. 1% of white dwarfs becomes SNIa and affect the planet habitability in a certain distance (Figure 4.3) (Gowanlock M. et al. 2011).

Fig.4.3 shows the surviving main sequence stars (distribution) from SN threats versus the galactic distance.

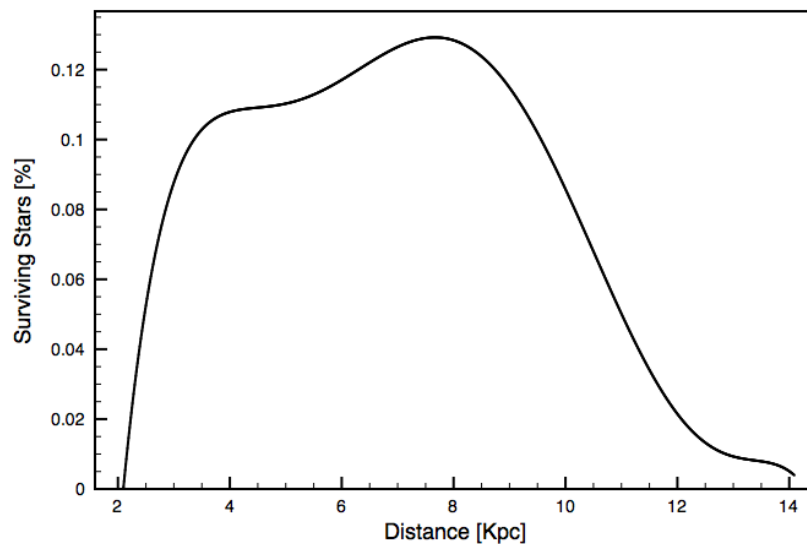


Figure 4.3: The SN surviving main sequence stars distribution versus the galactic distance (Besancon model)

The SN threats for habitable planets also have taken from Besancon model. Monte Carlo simulations shows, that a SN threat probability increases dramatically for the inner part of the Milky way, which agrees with Lineweaver C. et al. 2004 & Gowanlock M. et al. 2011, but SN threat density is not high enough to eliminate all the habitable planets.

We are using the assumption that there is at least one small planet per star

(Batalha N. M. et al. 2012). As a result, in our analysis we found a total 1.4 billion habitable planets (Monte Carlo simulations) in the Milky Way.

Figure 4.4 shows the limits of GHZ and the habitable planets candidates and figure 4.5 shows the total number of habitable planets and their density as a function of Galactic distance.

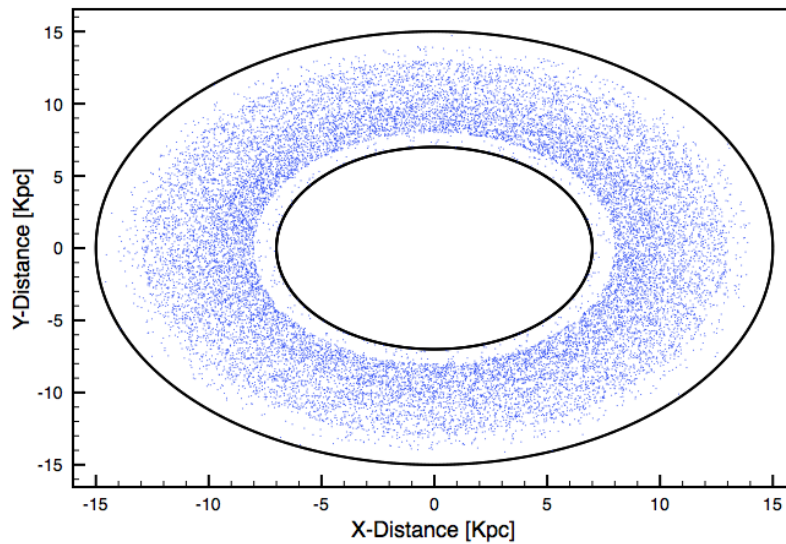


Figure 4.4: The GHZ limits and the habitable planet candidates.

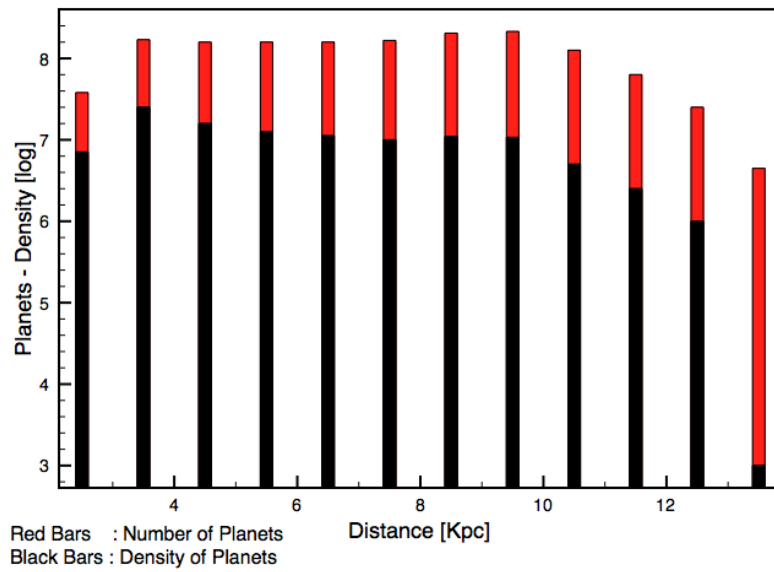


Figure 4.5: The final number of habitable planets (red bars), density (black bars).

## 4.8 Results

Our results indicate that there are 1.4 billion habitable planets in the Milky Way, which is 0,75% of the total star population, assuming 200 billion stars. The stellar distribution, stellar ages, spectral types, metallicities and distances were taken from the Besancon synthetic model. This number matches very well with Kepler results (42 candidates in the habitable zone until now versus 78 transiting habitable planets from our simulation).

# Chapter 5

## Conclusions

In the first section of this Diploma, we present a statistical analysis about existence of transiting extragalactic planets in Ursa Minor Dwarf spheroidal galaxy. We find that the probability to discover at least one transit in INT sample is  $58\% \pm 4\%$ . We consider this probability is the minimum of our magnitude range, assuming a bigger telescope gives out much bigger possibility. Considering JWST will be launched in the near future, RV follow up won't be a problem at all. So, we conclude that the possibility of finding a transit event like this is efficient nowadays.

In the second section of this Diploma we apply a statistical analysis of the Milky Way exoplanets using the Becanson galactic synthetic model to simulate the galactic and stellar habitable zones in order to calculate habitable planets. The stellar distribution, stellar ages, spectral types, metallicities and distances were taken from the Besancon synthetic model. To assess habitability on our Galaxy, we model supernova rates, planet formation and habitability on non-tidally locked planets. Our results indicate that there are 1.4 billion habitable planets in the Milky Way, which is 0,75% of the total star population, assuming 200 billion stars.



# Bibliography

- [1] Baltz E. A., Gondolo P. 1999, astro.ph, 9510B
- [2] Batalha N. M. et al. 2012, ApJS, 201, p.20
- [3] Borucki et al.1997, ASPC, 119, 153B
- [4] Borucki W., et al. 2012, ApJ, 745, p.120B
- [5] Charbonneau D. et al., 2002, ApJ, 568, 377C
- [6] Charbonneau D., Winn J. N., Latham D. W. et. al. 2006, ApJ, 636, 445
- [7] Deleuil et al. 1997, ASPC, 119, 259D
- [8] Deming D. et al., 2005, Nature, 434:740743,
- [9] Draper P. W., Gray N., Berry D. S., Taylor M. 2014, ascl.soft, 030, 24D
- [10] Gehrels N., et al. 2003, ApJ, 585, 1169G
- [11] Gilliland, R. L., Brown, T. M., Guhathakurta, P., et al. 2000, ApJ, 545, L47
- [12] Gonzalez, G., Brownlee D., 2001, Icar, 152, p.185G
- [13] Gowanlock M., Patton, D., McConnell S., 2011., AsBio, 11, p.855-873
- [14] Howard A. W. et al. 2012 ApJS, 201, 15H
- [15] Harrington J. et al., 2006, Science, 314:623626
- [16] Helmi A., White S. D. M., de Zeeuw P. T., Zhao H. 1999, Nature, 402, 53
- [17] Jones M. I., Jenkins J. S. 2014, A&A, 562A, 129J
- [18] Karachentsev I. D., Karachentseva V. E., Huchtmeier W. K., Makarov D. I. 2004, AJ, 127, 2031K

- [19] Kipping D. M. et al. 2012, ApJ, 750, 115K
- [20] Knutson H. A. et al., 2008, ApJ, 673, 526531
- [21] Lineweaver C., Fenner Y., Gibson B., 2004, Sci, 303, p.59L
- [22] Mandel K., & Agol E. 2002, ApJ, 580, L171
- [23] Mighell K. J., Burke Ch. J. 1999, AJ, 118, 366M
- [24] NASA/IPAC Extragalactic Database
- [25] Pál A. et. al. 2008, MNRAS, 390, 281
- [26] Prantzos N., 2008, Space Sci. Rev., 135, p.313-322
- [27] Robin A., Reyle C., Derrière S., Picaud S., 2003, A&A, 409, p.523-540
- [28] Seager S. & Mallen-Ornelas G. 2003, ApJ, 585, 1038
- [29] Seagroves S., Harker J., Laughlin G., et al., 2003, PASP, 115, p.1355-1362
- [30] Selsis F., et al., 2007, Icar, 191, p.453-468
- [31] Setiawan J., Klement R. J., Henning Th., et al. 2010, Sci, 330,1642S
- [32] Struve O. 1952, Obs, 72, 199S
- [33] Tinetti G. et al. 2012, ExA, 34, 311T
- [34] Zacharias N., Finch C. T., Girard T. M. et al. 2012, yCat, 1322, 0Z